

FEDSM2014-21161

CHARACTERIZING JETTING IN AN ACOUSTIC FLUIDIZED BED USING X-RAY COMPUTED TOMOGRAPHY

David R. Escudero* and Theodore J. Heindel
Department of Mechanical Engineering
Iowa State University
Ames, Iowa 50011

ABSTRACT

Understanding the jetting phenomena near the gas distributor plate in a fluidized bed is important to gas-solids mixing, heat and mass transfer, and erosion on any bed internals, which can all affect the performance of the bed. Moreover, acoustic vibration in a fluidized bed can be used to enhance the fluidization quality of particulate matter. Characterizing the jetting structure using X-ray computed tomography in a 3D fluidized bed, with and without acoustic intervention, is completed in this study. A 10.2 cm ID fluidized bed filled with glass beads, with material density of 2500 kg/m^3 and particles sizes ranging between 212-600 μm , is used in these experiments. X-ray computed tomography (CT) imaging is used to determine local time-average gas holdup. From this information, qualitative characteristics of the hydrodynamic structure of the multiphase flow system are determined. Local time-average gas holdup images of the fluidized bed under acoustic intervention at a high superficial gas velocity show that jets produced near the aeration plate merge with other jets at a higher axial position of the bed compared to the no acoustic condition. Acoustic fluidized beds also have a fewer number of active jets than the no acoustic fluidized bed, which allowed for a more homogeneous gas holdup region deep into the bed. Hence, the acoustic presence has a significant effect on the jetting phenomena near the distributor plate of the fluidized bed.

Keywords: Acoustic fluidized bed, hydrodynamics, jetting, X-ray computed tomography.

INTRODUCTION

Jetting has been studied extensively in the gas-solid fluidized bed literature; see for example Yang and Keairns [1], Ettehadieh et al. [2], Guo et al. [3, 4], Chen et al. [5], or Muller et al. [6]. However, most of the studies focused on jetting produced by using a central vertical nozzle or focused on jetting produced by a horizontal nozzle penetrating a lightly fluidized bed. There is limited information available from studies of jetting produced by the distributor plate of a fluidized bed, even though the hydrodynamics that are produced around this area are of extreme importance for the performance of the bed.

Yang [7] made a comparison of the vertical jetting phenomena between a 30 cm and a 3 m diameter fluidized bed. He studied the momentum dissipation, the jet penetration depth and the jet velocity profile by visual observation. He also proposed several correlations for the parameters studied above.

Wang et al. [8] calculated the volumetric solids holdup (inverse of gas holdup) of a bubbling gas-solid fluidized bed with a horizontal gas jet using electrical capacitance volume tomography (ECVT). They concluded that the solids holdup in the region of the gas-solid mixture jet is higher than that in the gas jet. Also, the penetration length of the horizontal gas solid mixture jet was larger than a horizontal gas jet alone.

Jet structure in a 3D fluidized bed was studied by Pore et al. [9] using nonintrusive techniques such as magnetic resonance imaging. They used different distributor plate configurations to study the jet-jet interactions, and the jet-wall interactions. They obtained maps of solid concentrations to investigate the jet stability under the different distributor configurations. They concluded that depending on the design of the distributor plate, the jets that are closer to each other are

*Corresponding Author: David Escudero (drescude@iastate.edu)

attracted. Likewise jets that are near the wall have a tendency to bend out towards the wall.

Guo et al. [10] studied the flow characteristics in a fluidized bed with jetting produced by a horizontal nozzle under acoustic assistance. They investigated the jet penetration depth and the particle concentration using an optical probe. They concluded that the jet penetration depth increased when an acoustic field of a certain sound pressure level and frequency was applied to the fluidized bed; they also concluded that sound waves have a different effect on particle concentration depending on the region of the bed.

Sound assisted fluidized beds have been studied in the literature because it has been shown that the inclusion of sound vibrations can help overcome fluidization problems in certain material types. Different behavior under sound vibrations have been observed by Leu et al. [11], Guo et al. [12], Kaliyaperumal et al. [13], Levy et al. [14], and Escudero and Heindel [15].

Visual observations as well as invasive techniques have been used to determine the different characteristics of the fluidized beds under the presences of acoustic waves [16, 17].

Noninvasive techniques have also been used to investigate the effects of acoustic waves on the void fraction distribution in fluidized beds. Escudero and Heindel [18] used X-ray computed tomography imaging to characterize the gas distribution in an acoustic gas-solid fluidized bed. They concluded that the addition of sound waves at a specific frequency and sound pressure level provided a more uniform particle distribution inside the bed. Moreover, they observed that the sound waves affected the jetting phenomena near the distributor plate.

X-ray imaging has been used to study multiphase fluidized systems for several years. They are a commonly employed noninvasive technique because they are safer than other nuclear based techniques (they can be turned on and off at will), have high resolution, and can be controlled by varying the voltage or current to improve penetration or contrast; there are other nonintrusive techniques (gamma ray computed tomography, electrical capacitance tomography, etc.), that can also be used to study the characteristics of multiphase flows.

Heindel et al. [19] developed an X-ray visualization facility to study different characteristics of opaque multiphase flows, from bubble columns to fluidized beds, with both good spatial and temporal resolution depending on the type of X-ray imaging technique used. Their facility is capable of utilizing three different X-ray imaging techniques: X-ray radiography, X-ray stereography, and X-ray computed tomography.

X-ray computed tomography (CT) generates a 3D density map (image) of the object of interest. X-rays pass through the object and the intensity values are recorded with an imaging device from several projections. After the images are collected, computer algorithms reconstruct the images to produce a 3D representation of the object. However, due to the large number of projections that must be acquired in order to obtain a whole reconstruction of the object, this technique does not have good temporal resolution. On the other hand, the multiple projections give a high spatial resolution to this technique, a characteristic

that can be used to determine the local time-average gas holdup in a very efficient way [20].

Local time-average gas or solid void fraction can be calculated using X-ray CT images. Using this information, Escudero and Heindel [20, 21] studied the effects of bed height, superficial gas velocity, and bed material on the local time-average gas holdup in a 10.2 cm fluidized bed. They determined that the fluidization hydrodynamics are affected by using different bed materials (glass beads, ground corncob, and ground walnut shell), superficial gas velocities (U_g), and height-to-diameter ratios (H/D).

Most of the studies on jetting have focused in the hydrodynamic distribution created by a single central or horizontal nozzle. The goal of this study is to focus on the jetting phenomena created by the distributor plate of an acoustic fluidized bed using images obtained via X-ray computed tomography.

EXPERIMENTAL SETUP

Certain aspects of the experimental setup are described in this section. A cylindrical, 10.2 cm diameter, cold flow sound assisted fluidized bed reactor is used in this study. To induce the acoustic vibration in the fluidized bed, a loudspeaker is located at the top of the fluidized bed. This speaker emits sine waves that are generated using a function generator at different frequencies with a specify amplitude controlled by a an amplifier, more details of the entire setup can be found in [15, 18].

The material used in these experiments is glass beads ($\rho_{\text{glass}} = 2500 \text{ kg/m}^3$), with particles sizes that range from 212 – 600 μm . The material is sifted several times using a mechanical shaker and sieves with different mesh sizes, to assure the material falls in the desired particle size range. The bed bulk density was determined using the material mass and the static bed volume. Bed material is slowly added until the desired static bed height is reached, which corresponds to $H/D = 0.5, 1$, and 1.5. Before the bed height is measured, the bed is fluidized and then allowed to collapse to avoid any packing effects due to the filling process. The material mass is then measured and the given bed bulk density is calculated. Table 1 summarizes the general bed characteristics.

TABLE 1: SUMMARY OF MATERIAL PROPERTIES.

| | Glass Beads | | |
|---|---------------------------|----------|------------|
| H/D | 0.5 | 1 | 1.5 |
| Bed Mass (g) | 620 | 1240 | 1860 |
| Bulk density (kg/m³) | 1505 | 1505 | 1505 |
| Diameter (μm) | 212-425, 425-500, 500-600 | | |
| Particle Density (kg/m³) | 2500 | | |
| U_{mf} no acoustic bed (cm/s) | 8.8 | 11 | 15 |
| U_{mf} acoustic bed (cm/s) | | | |
| 212-425 μm | 8.1 | 8.0 | 8.3 |
| 425-500 μm | 9.1 | 8.8 | 8.5 |
| 500-600 μm | 11.5 | 10.1 | 10.3 |

X-ray computed tomography (CT) scans are captured with and without acoustic intervention at different H/D ratios (0.5, 1,

1.5) and different superficial gas velocities $U_g = 1.5 U_{mf}$ and $3 U_{mf}$, where U_{mf} is the minimum fluidization velocity previously determined [15] (see also Table 1). The minimum fluidization velocity differs between the acoustic and the no acoustic fluidized bed.

The X-ray equipment used in this research is described in detail by Heindel et al. [19]; the procedure used for this study is described in detail by Escudero and Heindel [18].

To calculate the local time-average gas holdup information, data obtained from the CT reconstruction volume files are used. Gas holdup is the volumetric gas fraction present in the gas-solid fluidized bed, and is useful to characterize the hydrodynamic behavior of this multiphase flow system. Escudero and Heindel [18, 20] describe the mathematical equations used to quantify the local time-average gas holdup, ε_g ; the data obtained from that previous study are used to analyze the jetting phenomena that occurs near the distributor plate with and without acoustic intervention.

Using image analysis software, each of the volumetric pixels (voxels) in the gas holdup volume file are analyzed to determine the edge of each jet present inside the fluidized bed. To identify the jets, first, the voxel of interest is determined to be located inside the fluidized bed. Then, the center of the fluidized bed is located in the xy-plane. Once the center is located, the radius of the fluidized bed is determined (for the parameter of this study, the radius of the fluidized bed is equal to 86 voxels). Once the radius is determined, the next step is to ensure that the distance from the center of the bed to the voxel of interest is less than or equal to the radius of the bed.

To identify a jet, the gas holdup in a voxel of interest is compared to the neighboring local average gas holdup value. The local average gas holdup is determined by averaging the neighboring voxel gas holdup found in the same xy-plane and within a specified radius of the voxel of interest, making sure that only voxels that are within the fluidized bed are used in the average. The local average contains only voxels located in a single xy-plane because the vertically changing interface between the jet and the rest of the bed would otherwise skew the average. The average is localized so that sharp differences, such as that between a jet and the rest of the bed, are more clearly defined.

A circular area for the local average value is used because the jets are assumed to be roughly circular, and the bed is circular. The optimal radius for the local average area is approximately the distance from the center of a jet to the next closest jet. This is done to minimize the effect of the surrounding jets. If surrounding jets are included in the averaging region, a higher value of gas holdup can be obtained, skewing the average producing unfavorable results. Figure 1 demonstrates this principle; for this study the optimal radius is 18 voxels. The area inside the black circle is the region included in the average of the gas holdup values.

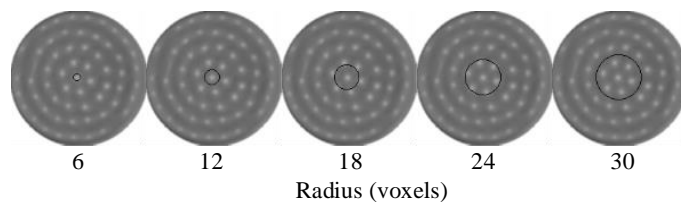


FIGURE 1: DIFFERENT RADIUS AVERAGING REGIONS FOR JET IDENTIFICATION. THE LIGHTER REGIONS INDICATE A HIGHER GAS HOLDUP, INDICATING A JET LOCATION.

Finally, if the gas holdup value of the voxel of interest is a specified threshold (12%) greater than the local average, it is marked as likely being located within a jet. Otherwise, it is left unmarked. Figure 2 shows y-slice planes at different thresholds for glass bead volume files. The threshold of 12% is chosen based on the number of voxels marked as a jet. Beyond the 12% threshold, the number of voxels marked as jets decrease, so there is no improvement in the identification of jets after this threshold.

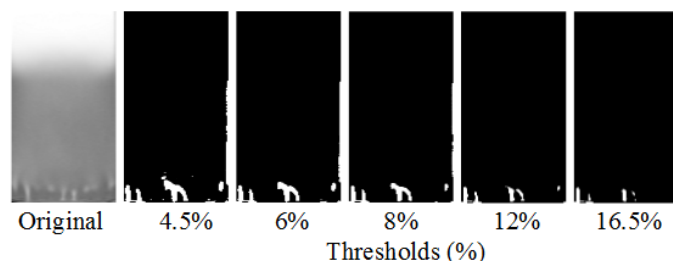


FIGURE 2: DIFFERENT THRESHOLD PERCENTAGES FOR GLASS BEADS.

To define individual jets, the image of the fluidized bed is assumed to be located in a 3D space such that the aeration plate is located in $z\text{-slice} = 0$ and all voxels have positive, integer values for all x , y , and z locations within the bed. The image is analyzed by looking at all the local voxel gas holdup values, compared to the local voxel average, in one xy-plane and then continuing to the next xy-plane.

Each jet is defined in a grouping of voxels that are determined to have a local gas holdup higher than the local average by a given threshold. For each voxel defined to be in a jet, it is first checked to see if the voxel of interest, labeled as (x, y, z) , is found adjacent to a jet grouping. If so, the voxel is added to the jet grouping. If not, a new jet group is defined starting with the voxel of interest.

Eventually, jets merge and lose their individual identities but are still strong enough to be considered jets. Therefore, the merged jets are divided so that a more accurate description of the jets can be given. In order to do this, the jets are assumed to have an approximate circular cross-section, and the center of each jet is calculated in each xy-plane. If an area of voxels that are marked as within a jet by the initial analysis is determined to be over the centers of more than one jet, the marked area is

divided such that the voxels closest to each jet center are added to that jet's group.

The initial analysis that defines which voxels are within jets will necessarily have some voxels marked as within jets that are not actually part of a jet. This "noise" is eliminated with filtering in the identification of individual jets. One filter through which the data are passed determines if the group of voxels identified as a jet begins at the aerator plate. If it does not, then the group of pixels is not a jet. If the number of identified jets is still higher than the number of aeration holes in the aeration plate, another filter successively removes the groups with the smallest number of voxels identified until the appropriate number of jets is established. It is assumed that the small number of voxels in the group indicates that the group is not a jet and is simply "noise" from the original analysis.

RESULTS AND DISCUSSION

Figure 3 shows different 2D y-slice images through the center of a fluidized bed of 500-600 μm glass beads with and without acoustic intervention for two different superficial gas velocities. The images in Figure 3 represent the original gas holdup volume file in grayscale next to the black and white image that is created using the jet identifier software. Note that only jets identified in this plane are visible, but in general, the entire 3D jet region is identified.

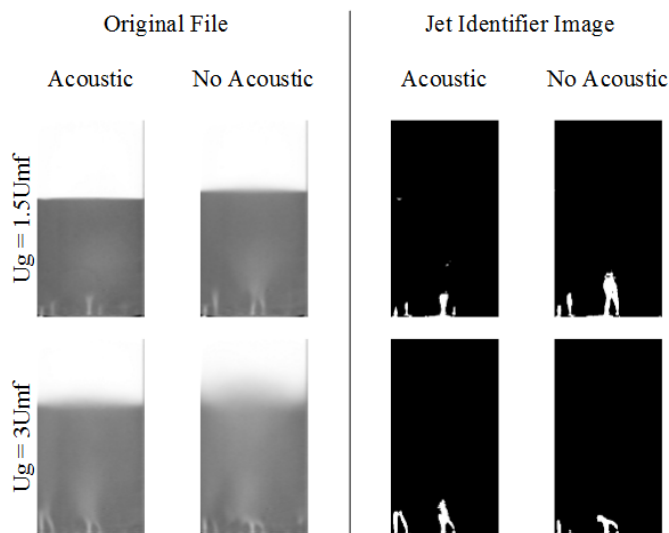


FIGURE 3: SINGLE SLICE IMAGES OF JETTING FOR 500-600 μm GLASS BEADS WITH AND WITHOUT ACOUSTIC INTERVENTION FOR $U_g = 1.5U_{mf}$ AND $U_g = 3U_{mf}$.

As Figure 3 shows for $U_g = 1.5U_{mf}$, the no acoustic fluidized bed condition exhibit larger jets that penetrate farther into the bed than the ones observed in the acoustic fluidized bed. Moreover, it shows that there are more jet-jet interactions in the no acoustic case, where jet merging is more prevalent. This phenomenon can also be observed in the original image.

As the superficial gas velocity increases to $U_g = 3U_{mf}$, jets become larger for the acoustic condition. This phenomenon is

attributed to the fact that as superficial gas velocity increases the effect of the acoustic vibrations is more prominent where the vibrations produced by the sound waves create paths where air can easily break through, allowing the jets to be larger in size than the jets produced without any acoustic excitation.

Different particle sizes were tested to compare the different effects, if any, that the acoustic vibration has on jetting when the particle diameter is changed while the superficial gas velocity remains constant at $U_g = 3U_{mf}$. As shown in Figure 4, the differences in jetting between the acoustic and the no acoustic case increase as the particle size increases. When the particle size is less than 500 μm , the differences are minimal. The same results were found in [18]. However, to fully understand and visualize the effects of acoustic vibration on the jetting phenomena, different 3D images of the jets produced by the aeration plate for both conditions were created and are presented below.

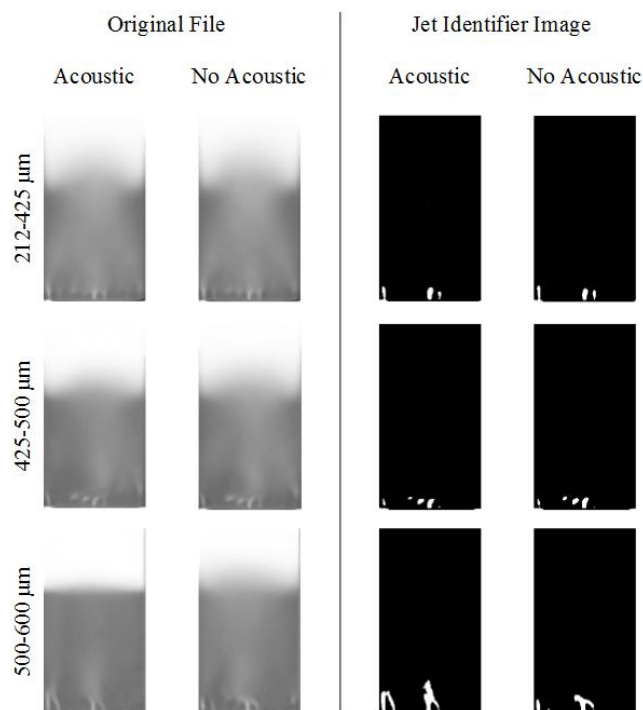


FIGURE 4: SINGLE SLICE IMAGES OF JETTING AT $U_g = 3U_{mf}$ FOR GLASS BEADS WITH DIFFERENT PARTICLE SIZE RANGES.

Figures 5 and 6 show 3D representations of the jets produced by the aeration plate for a bed of 425-500 μm glass beads with and without acoustic intervention, respectively. As shown for both conditions, the structure and length of the jets are similar, and the direction at which they extend in both images is also similar. It is interesting to see that four jets merge in the same location for both conditions. Figures 5 and 6 clearly show that for this particular particle size range and material, the addition of sound vibrations produces a negligible

change in the jetting phenomena in a fluidized bed. Similar results were observed in the smallest particle size range.

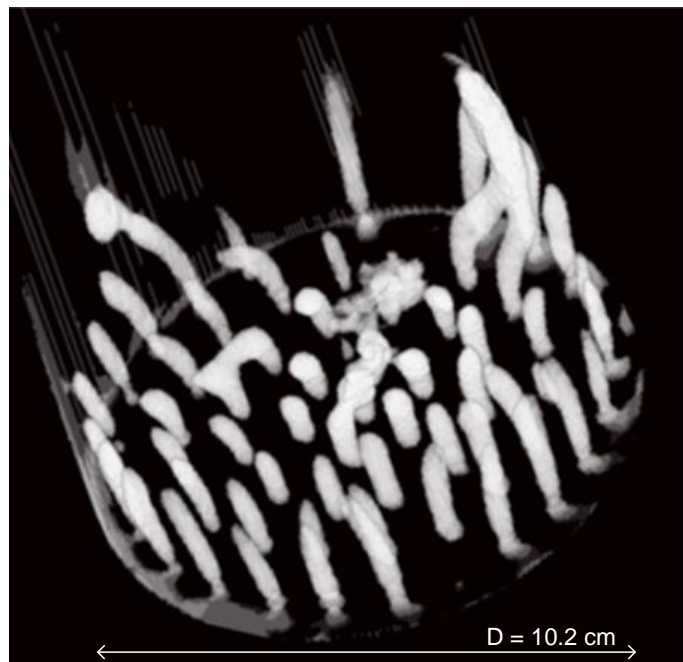


FIGURE 5: 3D IMAGE OF THE JETS FOR A FLUIDIZED BED OF 425-500 μm GLASS BEADS AT A $U_g = 3U_{mf}$ WITH ACOUSTIC INTERVENTION.

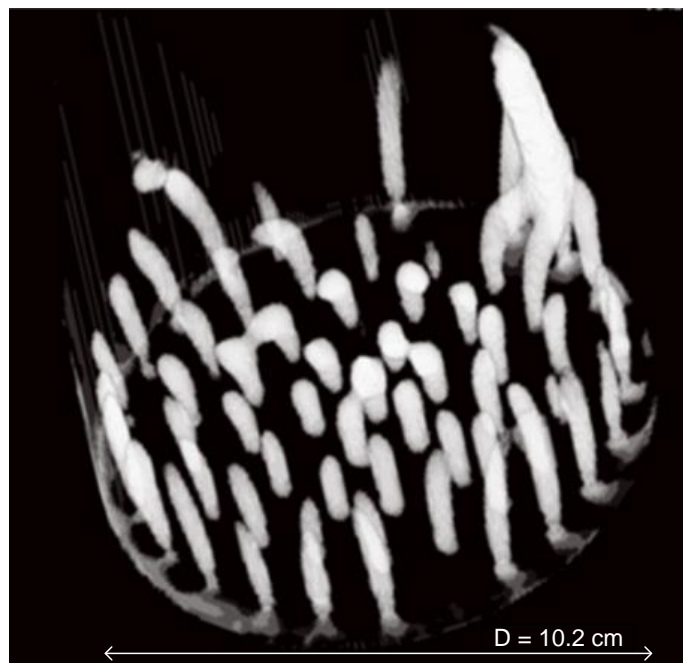


FIGURE 6: 3D IMAGE OF THE JETS FOR A FLUIDIZED BED OF 425-500 μm GLASS BEADS AT A $U_g = 3U_{mf}$ WITHOUT ACOUSTIC INTERVENTION.

Conversely, Figures 7 and 8 show the 3D representation of the jets for 500-600 μm glass beads. As Figure 7 shows when the fluidized bed has acoustic intervention the length of the jets appear to be longer than the same jets shown in Figure 8 without acoustic intervention particularly the jets that are located near the walls of the fluidized bed; corroborating the 2D images in Figures 3 and 4.

Moreover, these images show that for the acoustic case, there are less active jets present in the fluidized bed, some of the holes from the distributor does not show any jet formation compared to the same hole in the no acoustic case, this difference is attributed to the different superficial gas velocity that is applied to the fluidized bed.

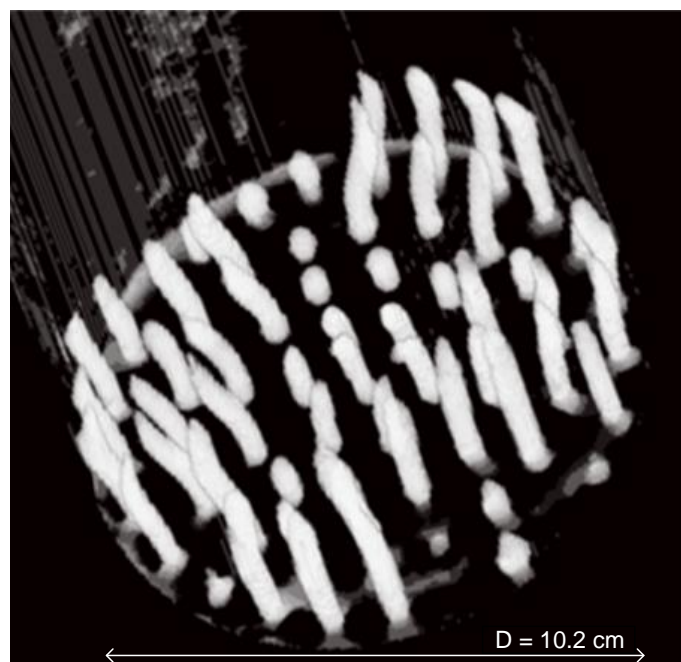


FIGURE 7: 3D IMAGE OF THE JETS FOR A FLUIDIZED BED OF 500-600 μm GLASS BEADS AT A $U_g = 3U_{mf}$ WITH ACOUSTIC INTERVENTION.

Future studies will explore the effects produced in jetting for different material types and also will obtain quantitative information, such as jet length penetration and expansion angle to quantify the effects of acoustic waves on jetting in gas-solid fluidized beds.

CONCLUSIONS

X-ray computed tomography was used to qualitatively identify features of the jetting phenomena produced by the distributor plate in a fluidized bed with and without acoustic sound vibrations.

Jets produced at higher superficial gas velocities near the distributor plate under the effect of acoustic vibration extend deeper into the bed material, merging with other jets at higher axial positions compared to the jets produced with no acoustic vibration.

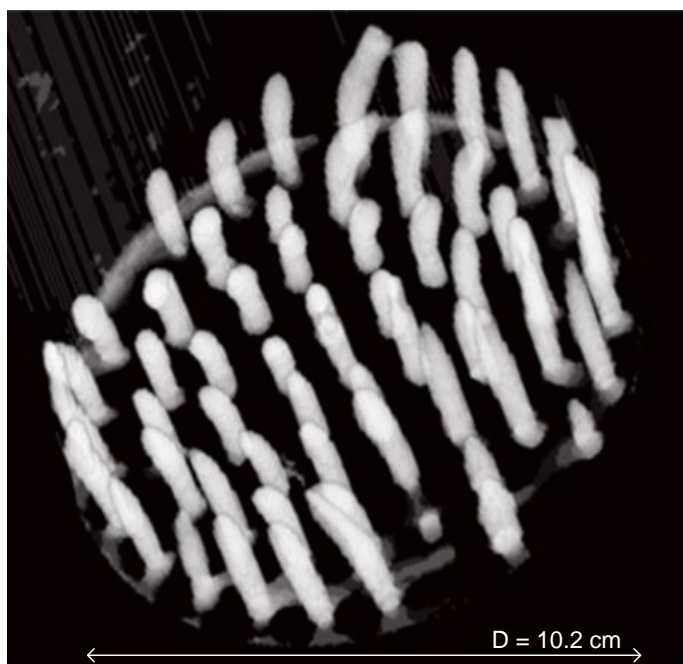


FIGURE 8: 3D IMAGE OF THE JETS FOR A FLUIDIZED BED OF 500-600 μm GLASS BEADS AT A $U_g = 3U_{mf}$ WITHOUT ACOUSTIC INTERVENTION.

Due to the difference in superficial gas velocity, which is a consequence of the presence of the acoustic waves, the acoustic fluidized bed presented less active jets in the bed with a particle size greater than 500 μm , therefore less jetting phenomena near the distributor than the no acoustic fluidized bed conditions is observed, allowing to have a better distribution of the void fraction throughout the entire fluidized bed.

ACKNOWLEDGMENTS

The X-ray facility used in this work was developed with support from the National Science Foundation under Grant No. CTS-0216367 and Iowa State University. This work in this study was supported through Iowa State University.

REFERENCES

- [1] Yang, W.-C. and Keairns, D. L., *A study of fine particles residence time in a jetting fluidized bed*. Powder Technology, 1987. **53**(3): p. 169-178.
- [2] Ettehadieh, B., Yang, W.-C., and Haldipur, G. B., *Motion of solids, jetting and bubbling dynamics in a large jetting fluidized bed*. Powder Technology, 1988. **54**(4): p. 243-254.
- [3] Guo, Q., Tang, Z., Yue, G., Liu, Z., and Zhang, J., *Flow pattern transition in a large jetting fluidized bed with double nozzles*. AIChE Journal, 2001. **47**(6): p. 1309-1317.
- [4] Guo, Q., Yue, G., Zhang, J., and Liu, Z., *Hydrodynamic characteristics of a two-dimensional jetting fluidized bed with binary mixtures*. Chemical Engineering Science, 2001. **56**(15): p. 4685-4694.
- [5] Chen, J., Lu, X., Liu, H., and Liu, J., *The effect of solid concentration on the secondary air-jetting penetration in a bubbling fluidized bed*. Powder Technology, 2008. **185**(2): p. 164-169.
- [6] Müller, C. R., Holland, D. J., Davidson, J. F., Dennis, J. S., Gladden, L. F., Hayhurst, A. N., Mantle, M. D., and Sederman, A. J., *Geometrical and hydrodynamical study of gas jets in packed and fluidized beds using magnetic resonance*. The Canadian Journal of Chemical Engineering, 2009. **87**(4): p. 517-525.
- [7] Yang, W.-C., *Comparison of jetting phenomena in 30-cm and 3-m diameter semicircular fluidized beds*. Powder Technology, 1998. **100**(2-3): p. 147-160.
- [8] Wang, F., Yu, Z., Marashdeh, Q., and Fan, L.-S., *Horizontal gas and gas/solid jet penetration in a gas-solid fluidized bed*. Chemical Engineering Science, 2010. **65**(11): p. 3394-3408.
- [9] Pore, M., Holland, D. J., Chandrasekera, T. C., Müller, C. R., Sederman, A. J., Dennis, J. S., Gladden, L. F., and Davidson, J. F., *Magnetic resonance studies of a gas-solids fluidised bed: Jet-jet and jet-wall interactions*. Particuology, 2010. **8**(6): p. 617-622.
- [10] Guo, Q., Si, C., and Zhang, J., *Flow characteristics in a jetting fluidized bed with acoustic assistance*. Industrial & Engineering Chemistry Research, 2010. **49**(16): p. 7638-7645.
- [11] Leu, L.-p., Li, J.-t., and Chen, C.-M., *Fluidization of group B particles in an acoustic field*. Powder Technology, 1997. **94**(1): p. 23-28.
- [12] Guo, Q., Liu, H., Shen, W., Yan, X., and Jia, R., *Influence of sound wave characteristics on fluidization behaviors of ultrafine particles*. Chemical Engineering Journal, 2006. **119**(1): p. 1-9.
- [13] Kaliyaperumal, S., Barghi, S., Zhu, J., Briens, L., and Rohani, S., *Effects of acoustic vibration on nano and sub-micron powders fluidization*. Powder Technology, 2011. **210**(2): p. 143-149.
- [14] Levy, E. K., Shnitzer, I., Masaki, T., and Salmento, J., *Effect of an acoustic field on bubbling in a gas fluidized bed*. Powder Technology, 1997. **90**(1): p. 53-57.
- [15] Escudero, D. and Heindel, T. J., *Minimum fluidization velocity in a 3D fluidized bed modified with an acoustic field*. Chemical Engineering Journal, 2013. **231**(0): p. 68-75.
- [16] Si, C. and Guo, Q., *Fluidization characteristics of binary mixtures of biomass and quartz sand in an acoustic fluidized bed*. Industrial & Engineering Chemistry Research, 2008. **47**(23): p. 9773-9782.
- [17] Herrera, C. A. and Levy, E. K., *Bubbling characteristics of sound-assisted fluidized beds*. Powder Technology, 2001. **119**(2-3): p. 229-240.
- [18] Escudero, D. R. and Heindel, T. J., *Acoustic fluidized bed hydrodynamics characterization using X-ray*

- computed tomography*. Chemical Engineering Journal, 2014. **243**(0): p. 411-420.
- [19] Heindel, T. J., Gray, J. N., and Jensen, T. C., *An X-ray system for visualizing fluid flows*. Flow Measurement and Instrumentation, 2008. **19**(2): p. 67-78.
- [20] Escudero, D., *"Bed height and material density effects on fluidized beds hydrodynamics"*, M.S. Thesis, Department of Mechanical Engineering. 2010, Iowa State University: Ames, IA. p. 109.
- [21] Escudero, D. and Heindel, T. J., *Bed height and material density effects on fluidized bed hydrodynamics*. Chemical Engineering Science, 2011. **66**(16): p. 3648-3655.